

The drinking water contaminant dibromoacetonitrile delays G1-S transition and suppresses Chk1 activation at broken replication forks

Caspari, Thomas; Dyer, James; Fenner, Nathalie; Dunn, Christian ; Freeman, Christopher

Scientific Reports

DOI:

[10.1038/s41598-017-13033-8](https://doi.org/10.1038/s41598-017-13033-8)

Published: 01/01/2017

Peer reviewed version

[Cyswllt i'r cyhoeddiad / Link to publication](https://doi.org/10.1038/s41598-017-13033-8)

Dyfyniad o'r fersiwn a gyhoeddwyd / Citation for published version (APA):

Caspari, T., Dyer, J., Fenner, N., Dunn, C., & Freeman, C. (2017). The drinking water contaminant dibromoacetonitrile delays G1-S transition and suppresses Chk1 activation at broken replication forks. *Scientific Reports*, 7, [12730]. <https://doi.org/10.1038/s41598-017-13033-8>

Hawliau Cyffredinol / General rights

Copyright and moral rights for the publications made accessible in the public portal are retained by the authors and/or other copyright owners and it is a condition of accessing publications that users recognise and abide by the legal requirements associated with these rights.

- Users may download and print one copy of any publication from the public portal for the purpose of private study or research.
- You may not further distribute the material or use it for any profit-making activity or commercial gain
- You may freely distribute the URL identifying the publication in the public portal ?

Take down policy

If you believe that this document breaches copyright please contact us providing details, and we will remove access to the work immediately and investigate your claim.

The drinking water contaminant dibromoacetonitrile delays G1-S transition and suppresses Chk1 activation at broken replication forks

Thomas Caspari^{1*}, James Dyer^{1,2}, Nathalie Fenner², Christian Dunn² and Chris Freeman²

1: Bangor University, School of Medical Sciences, Bangor LL57 2UW, United Kingdom

2: Bangor University, Bangor Wetlands Group, School of Biological Sciences

* Corresponding Author: Dr Thomas Caspari, Bangor University, School of Medical

Sciences, Bangor LL57 2UW, United Kingdom, email: t.caspari@bangor.ac.uk; phone

0044-(0)-1248382526

Classification: BIOLOGICAL SCIENCES/Cell Biology

ORCID iD numbers: orcid.org/0000-0002-1450-4774

Key words: haloacetonitrile, dibromoacetonitrile, Chk1, cell cycle, DNA replication

Abstract

Chlorination of drinking water protects humans from water-born pathogens, but it also produces low concentrations of dibromoacetonitrile (DBAN), a common disinfectant by-product found in many water supply systems. DBAN is not mutagenic but causes DNA breaks and elevates sister chromatid exchange in mammalian cells. The WHO issued guidelines for DBAN after it was linked with cancer of the liver and stomach in rodents. How this haloacetonitrile promotes malignant cell transformation is unknown. Using fission yeast as a model, we report here that DBAN delays G1-S transition. DBAN does not hinder ongoing DNA replication, but specifically blocks the serine 345 phosphorylation of the DNA damage checkpoint kinase Chk1 by Rad3 (ATR) at broken replication forks. DBAN is particularly damaging for cells with defects in the lagging-strand DNA polymerase delta. This sensitivity can be explained by the dependency of pol delta mutants on Chk1 activation for survival. We conclude that DBAN targets a process or protein that acts at the start of S phase and is required for Chk1 phosphorylation. Taken together, DBAN may precipitate cancer by perturbing S phase and by blocking the Chk1-dependent response to replication fork damage.

Introduction

Dibromoacetonitrile (DBAN) is generated at low nanomolar concentrations when bromide reacts with nitrogenous organic matter during the chlorination of drinking water¹. A survey of 20 water supply systems in England and Wales revealed DBAN as the most abundant haloacetonitrile (HAN) (≤ 40.2 nM, ≤ 8 μ g/L)². Epidemiological studies in the USA linked the consumption of chlorinated water with an increased risk in bladder, brain and rectal cancer^{3 4 5}. Very high concentrations of DBAN (> 250 μ M) induce cancer of the liver and stomach in rodents^{6 7}. The WHO issued guidelines for DBAN (0.35 μ M), dichloroacetonitrile (DCAN; 0.18 μ M) and trichloroacetonitrile (TCAN; < 0.007 μ M) in the response to these findings⁸.

While DBAN is probably not mutagenic, it effectively alkylates DNA *in vitro* which may explain how it breaks DNA and elevates sister chromatid exchange in yeast and mammalian cells^{9 10 11}. DBAN increases the levels of reactive oxygen species (ROS) in rat cells as indicated by a rise in 8-hydroxy-2-deoxyguanosine (8OHdG)^{12 13} and blocks aldehyde dehydrogenase¹⁴, dimethylnitrosamine-demethylase¹⁵, glutathione-S-transferase¹⁶, superoxide dismutase and catalase¹⁷ in the liver. Monobromoacetonitrile (BAN) was shown to induce endoreplication in Chinese hamster ovary cells by blocking mitosis¹⁸. While these findings indicate a potential health risk, it is still unclear how DBAN precipitates cancer.

Using the model organism fission yeast (*Schizosaccharomyces pombe*), we report here that DBAN delays G1-S transition and specifically blocks the activation of the DNA damage checkpoint kinase Chk1 at broken DNA replication forks.

The replication machinery assembles around the DNA helicase MCM₂₋₇ at dedicated chromosomal sites (origins) in a stepwise process (reviewed in¹⁹). The pre-replication

complex forms late in G1 when DDK, a heterodimer of Cdc7/Hsk1 kinase and its activating subunit Dbf4/ASK, recruits Sld3 (Treslin) and Cdc45. The cell cycle regulator CDK (cyclin-dependent kinase) activates this complex later at the start of S phase by loading the BRCT-domain protein Rad4 (Dbp11, TopBP1), Sld2, DNA polymerase epsilon and the GINS proteins²⁰. When DNA polymerase alpha-primase and MCM10 associate with this structure, processive DNA replication begins. The lagging strand is displaced in front of the moving replication fork where Cdc45 channels it into DNA polymerase delta. The leading strand runs straight through the fork where it is copied by DNA polymerase epsilon^{21 22}. A drop in the nucleotide pool, which can be triggered by the RNR (ribonucleotide reductase) inhibitor hydroxyurea (HU), stalls forks in early S phase by activating the intra-S checkpoint kinase Cds1²³. Cds1 binds to Mrc1 (Claspin) at the stalled fork after both proteins were phosphorylated by Rad3 (ATR)²⁴. Mrc1 associates also with early origins during the G1-S transition, independently of the checkpoint, where it is modified by DDK²⁵. The collision of replication forks with immobilised topoisomerase 1, which can be trapped on the DNA by camptothecin (CPT), triggers the phosphorylation of the DNA damage checkpoint kinase Chk1 at serine 345 by Rad3²⁶. Activation of Cds1 and Chk1 block both the cell cycle activator Cdc2 (CDK1) thereby initiating a transient G2-M arrest²⁷. We report here that DBAN perturbs G1-S transition and blocks Chk1 phosphorylation at a broken replication fork without affecting the Rad3-dependent modification of other checkpoint proteins. DBAN may therefore act on a process or a protein that is required at the start of S phase and later at damaged DNA replication forks. We conclude that DBAN elicits DNA replication stress, a known driver of cancer development²⁸.

Results

DBAN interferes with S phase

Informed by the ability of bromoacetonitrile (12 μ M) to block mitosis in Chinese hamster ovary (CHO) cells¹⁸, we first tested whether haloacetonitriles (HANs) impact on cell cycle progression. Wild type cells were synchronised in G2 by lactose gradient centrifugation²⁹ and released into medium with 10 μ M bromo-, dibromo-, chloro-, dichloro- or trichloroacetonitrile (BAN, DBAN, CAN, DCAN, TCAN). Samples were withdrawn every 20min to score septated G1/S cells. While the monohalogen compounds, BAN and CAN, allowed cells to complete two cell cycle rounds, their dihalogen forms, DCAN and DBAN, delayed entry into the second cycle by 40min and 60min, respectively (figure 1c, d). Unlike CHO cells¹⁸, DBAN-treated yeast cells arrested in G2 before the onset of mitosis (figure S1a, b). Since a second cycle G2 arrest is typical for drugs like hydroxyurea (HU) or camptothecin (CPT) that interfere with DNA replication, we concluded that DBAN and DCAN perturb S phase thereby triggering the G2 delay (figure 1g). HU stalls DNA replication forks by depleting the dNTP pool, whereas CPT breaks forks by immobilising topoisomerase 1 in front of the advancing replication complex. Both events delay onset of mitosis through the Rad3-dependent activation of the checkpoint kinases Cds1 and Chk1, respectively^{27 30}. To investigate whether the DBAN-induced S phase perturbations activate the checkpoint, we synchronised a checkpoint-defective $\Delta rad3 \Delta tel1$ double mutant (Tel1/ATM is the second checkpoint kinase besides Rad3/ATR) in G2 and released cells into medium with or without 10 μ M DBAN. Very unexpectedly, the checkpoint deficient strain arrested for longer compared to wild type cells (figure S1c) showing that the delay is checkpoint-independent. The second unexpected observation was made when we analysed the cell cycle impact of trichloroacetonitrile. Unlike DBAN or

DCAN, TCAN (10 μ M) blocked entry into the first cycle for around 280 min (figure 1e). Since such a first cycle arrest is typical for agents that break DNA³⁰ and because HANs were linked with DNA breaks in mammalian cells¹⁰, we tested whether they increase the phosphorylation of histone H2AX at S129 by Rad3 and Tel1, an established marker of chromosomal breaks³¹. Intriguingly, all HANs (BAN, CAN, DBAN, TCAN), with the exception of DCAN, reduced the phosphorylation of H2AX showing that DNA breaks are not the cause of the arrest (figure S1d). Since H2AX is also phosphorylated early during unperturbed S phase³¹, this drop may be caused by depleting the pool of S phase cells due to the G2 arrest. We can however not exclude the possibility that the HANs affect the H2AX phosphorylation directly since BAN and CAN do not show a strong arrest (figure 1a, b). The decline in H2AX phosphorylation was concentration dependent starting at 8 μ M DBAN (figure S1e). We next tested whether the first cycle arrest is unique to TCAN and found that a higher concentrations of DBAN (20 μ M) also delayed cells in the first G2 phase (figure 1f). This implies that TCAN is more effective than DBAN in eliciting this response. As in the case of the second cycle arrest, the DNA damage checkpoint was not required (figure S1f). A checkpoint-defective *$\Delta cds1 \Delta chk1$* double mutant delayed mitosis for 220min, although this arrest was 40min shorter compared to wild type cells (figure S1f). We did not further investigate this first cycle arrest as we wanted to learn more about how DBAN perturbs S phase given the importance of DNA replication stress in malignant transformation²⁸.

DBAN delays G1-S progression

To map the execution point of DBAN in S phase, wild type cells were enriched in G1 by nitrogen starvation and released back into the cell cycle by replenishing the medium with a nitrogen source²⁹. The DNA content was measured by flow cytometry over 8 hours to

monitor progression from G1 (1 copy of the chromosomes, 1C) into G2 (two copies, 2C) (figure 2). While most untreated cells reached G2 4h post-release (figure 2a), DBAN and TCAN (10 μ M) treated cells retained a 1C DNA content (figure 2b). We also blocked cells in early S phase with 15mM HU to have an internal marker for unreplicated DNA (figure 2b, c). Eight hours after the release from G1, only HU and TCAN treated cells remained arrested, while DBAN permitted the completion of DNA replication (figure 2c). This shows that DBAN only delays G1-S transition, whereas TCAN blocks this step more effectively. None of the other HANs (BAN, CAN, DCAN) had a similar effect, although cells had a slightly larger DNA content at the 8h time point compared to untreated cells (figure 2c). This difference indicates that untreated cells had re-entered the cell cycle as this would average their DNA content at a slightly lower value, while CAN and DCAN treated cells remained in G2 for longer with the full 2C DNA content. To exclude the possibility that the G1 arrest protocol impacts on this interesting finding, we synchronised *nda3-KM311* cells in mitotic prophase. This cold sensitive beta-tubulin mutant stops with condensed chromosomes without a mitotic spindle at 20°C and returns to the cell cycle within minutes upon a temperature up-shift to 30°C³². In line with the first experiment, TCAN prevented the accumulation of G2 cells whereas DBAN only delayed it (figure S1g). We next arrested cells in early S phase by incubating a wild type strain in 15mM HU for 3.5h²⁹ to test whether DBAN or TCAN (10 μ M) would impact on DNA replication. While the latter was not the case for DBAN, TCAN-treated cells delayed for 20min compared to untreated cells (figure S2c). Since DNA replication was complete within 60min in the absence of TCAN, a 20min difference (1/3 of S phase) may well be significant. Taken together, these data show that DBAN delays G1-S transition, but allows cells to complete DNA replication. In contrast, TCAN blocks cells effectively before the G1-S

transition and delays DNA replication. This conclusion is in line with the higher potency of TCAN as a G2 blocker (figure 1e).

DBAN affects DNA polymerase delta

Since DBAN allows DNA replication to proceed after an initial G1-S delay (figure 2c, S1g), we tested whether this affects the three replicative DNA polymerases, alpha (Pol1, *swi7*), epsilon (Pol2, *cdc20*) or delta (Pol3, *cdc6*). Since these essential genes cannot be deleted, we used temperature-sensitive mutants at the semi-restrictive temperature of 30°C. Serial dilutions of the strains were applied to rich medium plates containing no HAN or 10µM DBAN. We also incubated one plate at 37°C to confirm the temperature sensitivity. While mutations in the three essential subunits of Pol delta (*cdc6.23* [catalytic], *cdc27.P11* [non-catalytic], *cdc1.P13* [non-catalytic]) impaired cell viability, mutations in the catalytic subunits of Pol epsilon (*cdc20.M10*) or Pol alpha (*swi7.H4*) did not (figure 3b). Interestingly, deletion of the fourth, non-essential Pol delta subunit, *cdm1*, had also no effect (figure 3c). We next tested mutations in the MCM₂₋₇ helicase that unwinds the DNA template (MCM2 [*cdc19.P1*], MCM4 [*cdc21-M68*] or MCM5 [*nda4-108*]), but failed to detect loss of viability (figure 3c). Also no impact on cell growth was found for mutations in DDK (Cdc7/Hsk1) kinase (*hsk1-1312*) and in the replication factor Rad4 (TopBP1) (*rad4.116*) (figure 3c). Whether a mutation in Ctf4 (*mcl1-1*), which binds Pol alpha to the replication complex, impairs cell viability was difficult to judge since the strain grew very poorly even in the absence of DBAN (figure 3b). Interestingly, none of the DNA pol delta mutants showed a growth defect on TCAN plates even at 20µM (figure 3d). This was unexpected given the high impact of TCAN on cell cycle progression. A possible explanation is provided by the replication delay caused by TCAN (figure S2c) that may prevent loss of viability. The pol delta mutants were also not sensitive to CAN, BAN or

191 DCAN at 10 μ M (figure 3e).

192

193 **DBAN overcomes the intra-S arrest of a pol delta mutant**

194 To find out why pol delta mutants are DBAN sensitive, we synchronised wild type, pol
195 alpha (*swi7.H4*), pol delta (*cdc27.P11*) and pol epsilon (*cdc20.M10*) strains in early S
196 phase using the HU arrest protocol ²⁹. After HU was washed out, cells were released into
197 medium with or without 10 μ M DBAN. Flow cytometry showed that untreated wild type cells
198 completed S phase within 60min (figure 4a). As previously reported ³³, the untreated
199 mutant strains delayed S phase progression at the semi-permissive temperature of 30°C
200 (figure 4b-d). While DBAN had no impact on S phase within the first 60min in the case of
201 the pol alpha and pol epsilon mutants, it did significantly advance DNA replication of the
202 pol delta (*cdc27.P11*) strain (figure 4c). This advancement was clearly detectable at the
203 60min and 90min time points (figure 4c). After 2h, the DBAN-treated *cdc27.P11* cells
204 initiated already the next cell cycle round compared to the untreated sample (figure 4c).
205 Cdc27 connects the catalytic (Cdc6) and non-catalytic (Cdc1) subunits, and binds Pol
206 delta to the DNA sliding clamp PCNA ³⁴. DBAN also advanced DNA replication of the
207 other two mutant strains but later and to a lesser extend (figure 4b, d).

208 These results imply that DBAN abolishes the intra-S phase arrest of the pol delta
209 (*cdc27.P11*) strain, which may be linked with its loss of viability on DBAN plates (figure
210 3b). Since the viability of pol delta mutants depends on Chk1 kinase ³³, we next tested
211 whether DBAN interferes with the activation of the checkpoint kinases Cds1 and Chk1.

212

213 **DBAN suppresses the activation of Chk1**

214 To find out whether DBAN perturbs activation of the intra-S checkpoint kinase Cds1 at
215 stalled forks, asynchronous *cds1-His₆HA₂* cells ³⁵ were incubated with 10 μ M DBAN, 12mM

HU or with both chemicals simultaneously for 4h. Total protein extracts were loaded onto a 6% phos-tag SDS gel to assay the phosphorylation status of Cds1. Phostag electrophoresis reveals the phosphorylation pattern of proteins as their mobility is inversely related to the extent of their modification³⁶. While DBAN did not promote the modification of Cds1, the kinase was intensively phosphorylated when DNA replication forks stalled in the presence of HU. Although DBAN did not impact on this hyperphosphorylation, it induced a faster migrating band (figure 5a). The latter band could be a hypophosphorylated form of Cds1.

We then repeated this experiment with a *chk1-HA₃* strain³⁷ but replaced HU with 12μM camptothecin (CPT) to break DNA replication forks. In contrast to Cds1, DBAN effectively suppressed Chk1 phosphorylation at serine 345 (figure 5b). On normal SDS page, S345 phosphorylation was detected as a band shift, as previously reported, which disappeared upon DBAN exposure (figure 5b, lower panel)³⁷. DBAN also induced very slowly migrating, hyperphosphorylated bands independently of CPT. The suppression of Chk1 phosphorylation at damaged replication forks could explain why DBAN impairs the viability of DNA polymerase delta mutants which rely on this kinase for survival (figure 3b).

To test whether DBAN is an inhibitor of Rad3 kinase, we replaced CPT with MMS (methyl-methanesulfonate) that damages DNA by alkylation³⁸. Since DBAN did not block the MMS-induced phosphorylation of Chk1 (figure S1h), it is unlikely that the HAN impairs Rad3 kinase directly. We then exposed wild type cells (*chk1-HA₃*) to CPT or to the combination of DBAN and CPT on plates to gauge whether replication forks still break. The latter seems to be the case as DBAN rendered wild type cells (*chk1-HA₃*) CPT sensitive (figure 5d). This increase in sensitivity, which was similar to the sensitivity of a kinase-dead *chk1* mutant (*chk1-D155E-HA₃*), indicates that forks still break while DBAN prevents activation of Chk1.

To find out when DBAN acts on Chk1 in the cell cycle, we synchronised *chk1-HA₃* cells in early S phase with HU and released them into medium with CPT (12µM) or with CPT and DBAN or TCAN (10µM). In line with the idea that Chk1 is activated once bulk DNA synthesis had been completed³⁹, the shift band of Chk1, indicative of serine 345 phosphorylation, appeared 60 min post-release after the levels of the DNA replication marker Mrc1 had declined (figure 5e)²⁴. Since Chk1 is weakly phosphorylated during the HU arrest, all samples displayed a weak shift band that increased strongly when forks were damaged by CPT (figure 5e, bottom panel). The presence of DBAN or TCAN effectively suppressed activation of Chk1 (figure 5f). Since Rad3 modifies also the Rad9 subunit of the 9-1-1 checkpoint ring at broken forks (figure 5c)⁴⁰, we repeated this experiment with a HU-synchronised *rad9-HA₃* strain⁴¹. As in the case of Chk1, Rad9 phosphorylation is detectable as a band shift. This shift was not affected by DBAN strongly suggesting that Chk1 is specifically targeted by the haloacetonitrile (figure 5g). We noticed however that the Rad9 phosphorylation peaked 30 min earlier in the presence of DBAN (figure 5g, panels 3+4). The phos-tag assay did not reveal any changes in the Rad9 phosphorylation pattern which were DBAN specific (figure S1i). Collectively, these results suggest that DBAN kills pol delta mutants (figure 3b) and renders wild type cells sensitive to camptothecin (figure 5d) by preventing the phosphorylation of Chk1 at damaged DNA replication forks.

Discussion

The evidence presented here reveal novel activities of DBAN at two stages during the cell cycle, at the G1-S transition and later at damaged replication forks (figure 6). DBAN affects both processes in a negative way as it delays entry into S phase (figure 2) and suppresses phosphorylation of Chk1 (figure 5b, f) without affecting the activation of Rad9 (figure 5g) or Cds1 (figure 5a). Replication fork damage can originate from the inhibition of topoisomerase 1 by camptothecin or from mutations in the lagging strand DNA polymerase delta^{26 33}. Collectively, these findings imply that DBAN blocks an event or a protein that is required for both, entry into S phase and activation of Chk1 at damaged forks (figure 6). Early in S phase, human and yeast cells phosphorylate the histone H2AX in a cell cycle specific manner independently of DNA breaks^{31 42}. The same chromatin modification is later required for the recruitment of Crb2 (53BP1) to a broken fork where the scaffold protein associates with Chk1^{43 44}. DBAN and TCAN may therefore compromise both processes by reducing H2AX phosphorylation (figure S1d,e). For example, the HANs may up-regulate a phosphatase, like human PP2A-B56c, that dephosphorylates H2AX at a damaged forks upon CPT treatment⁴⁵. What argues against this model is the survival of the DNA pol delta mutants in the presence of BAN, CAN or TCAN (figure 3) which all reduce H2AX phosphorylation (figure S1d). An alternative explanation is provided by the dual function of Rad4/Cut5 (TopBP1) during G1-S transition and in the activation of Chk1^{46 47}. Rad4 associates with Sld3 and Sld2/Drc1 at start and with Crb2 at broken DNA^{44 46}. What argues however against Rad4 is its requirement for the activation of Cds1 at stalled forks⁴⁷ which is not affected by DBAN (figure 5a). A third candidate is DDK kinase as it initiates the assembly of the replication complex at the end of G1 (reviewed in¹⁹) and terminates Chk1 activation by phosphorylating the Rad9 subunit of the 9-1-1 complex⁴⁸. We have however not found any evidence that the Rad9

phosphorylation pattern changes upon DBAN exposure (figure S1i). A fourth possibility is provided by Mrc1 (Claspin) that associates with early replication origins at start²⁵ and recruits human Chk1 to broken forks⁴⁹. A similar interaction between *S.pombe* Chk1 and Mrc1 has not yet been reported. Finally, DBAN may act directly on Chk1 as indicated by its hyper-phosphorylation (figure 5b). Chk1 is required in *S.pombe* and human cells at the start point of the G1-S transition^{50 51} and at broken forks²⁶. Further work will however be required to dissect these different possibilities that are of great interest as it still enigmatic why human Chk1 occupies a dominant role in S phase whereas yeast Chk1 appears to act mainly in G2 (figure 5e)³⁹.

DBAN is known to block a large number of enzymes *in vitro*⁷ but it is as yet unclear how it interacts with proteins. Halogen atoms like bromine and chlorine have a positive charge, known as the alpha-hole that can make electrostatic contacts with the protein backbone or amino acid side chains⁵². While bromine interacts preferentially with the side chain of arginine, chlorine prefers leucine⁵³. Whether this explains why TCAN is a stronger cell cycle inhibitor than DBAN (figure 1) is difficult to tell as it is unclear to which protein they bind. It is even not entirely safe to conclude that they bind to the same protein. DBAN and TCAN behave in a similar way regarding the G1-S delay (figure 2) and the inhibition of Chk1 phosphorylation (figure 5f). Both HANs differ however in their lethality when DNA polymerase delta is mutated (figure 3d). Although this appears to contradict the earlier notion that DBAN kills these mutant strains by blocking Chk1 phosphorylation at damaged forks, it could be explained by the ability of TCAN to delay DNA replication (figure 4c). If this delay were to prevent fork damage in pol delta mutant cells, the inhibition of Chk1 would not affect cell viability.

Although DNA replication stress is a good explanation for why DBAN (10µM) triggers a second cycle delay (figure 1d), it would not provide an answer to why 20µM DBAN block

cells in the first G2 (figure 1f). The concentration dependency implies that DBAN has either more than one target in cells with different affinities for the HAN or that DBAN upregulates the expression or activity of a protein in a concentration dependent manner. From the different options discussed earlier, the up-regulation of a phosphatase like PPA2 would connect the diverse cell cycle activities of DBAN and TCAN. Interestingly, induction of PPA2 arrest cells in G2 independently of the DNA damage checkpoint when the accessory protein Vpr of human immunodeficiency virus type 1 (HIV-1) is over-expressed in *S.pombe*⁵⁴. Since this arrest shares a similar independence from the Rad3-Tel1 checkpoint as the G2 arrest produced by DBAN and TCAN (Figure 1e,f, S1f), it is quite possible that both HANs delay cell cycle progression in G2 through a mechanism that involves the activation of a phosphatase acting on the cell cycle machinery.

The final point to consider is whether DBAN, which is frequently found in water supply systems², poses a serious cancer risk. The concentration of 10µM used in this study is approximately 30 times higher than the WHO guideline of 0.35µM (70µg/L). It is therefore unlikely that DBAN levels reach such high concentrations in tap water. The peak concentration found in water supply systems in Western Australia, for example, was 0.13µM (26.6µg/L)⁵⁵, whereas the peak value in the United Kingdom was with 0.04µM (8µg/L) much lower². It is however not yet clear whether haloacetonitriles accumulate over a longer consumption period in the liver, gastrointestinal tract or the kidneys⁷. The latter may explain why the consumption of chlorinated drinking water was linked with cancer³.

Materials and Methods

Yeast Strains

The genotype of the strains used in this study is *ade6-M210 leu1-32 ura4-D18*. Wild type cells contained no additional mutation and the different mutant alleles are mentioned in the text. The *cds1-HA₂His₆ [URA4+]* *ura4-D18* strain is described in ³⁵ and the *chk1-HA₃* strain in ³⁷. Before cells were synchronised in G1 by nitrogen starvation, all auxotrophic markers were crossed out.

Cell synchronisation

Cells were synchronised as described in ²⁹. HU was used at a final concentration of 15mM for 3.5h at 30 °C in rich medium. For the G1 arrest, cells without auxotrophic markers were first grown in minimal medium with nitrogen before being transferred to minimal medium without nitrogen for 16h at 30°C. Lactose gradients were centrifuged for 8min at 800rpm. The *nda3.KM311* mitotic arrest was performed in rich medium as reported in ⁵⁶.

Flow cytometry

The DNA content was measured using a CUBE 8 (Sysmex) instrument as described in ²⁹. The histograms were produced using the free Flowing Software (<http://flowingsoftware.btk.fi/>)

Phos-tag SDS page

Phostag gels (6%) were prepared and run as reported in ⁵⁷.

Antibodies

Anti-HA antibody (BioSource, Covance MMS-101P-200), anti-Mrc1 antibody (ABCAM, ab188269), anti-Cdc2 antibody (ab5467) and anti-Histone 2AX-S129-P antibody

365 (ab17576). Secondary mouse-HRP (Dako, P0447), secondary rabbit-HRP (Dako, P0217).

366

367 **Protein extracts**

368 Total protein extracts were prepared as described in ⁴¹

369

370 **Chemicals**

371 Bromoacetonitrile (Sigma Aldrich, 242489), dibromoacetonitrile (Alfa Aesar, A16994),

372 chloroacetonitrile (Sigma Aldrich, C19651), dichloroacetonitrile (Alfa Aesar, A10612),

373 trichloroacetonitrile (Sigma Aldrich, T53805), phostag-acrylamide (AlphaLabs, AAL-107,

374 300-93523), hydroxyurea (Formedium, HDU0025).

375

Figure Legends

Figure 1. Dibromoacetonitrile (DBAN) arrests cell cycle progression in a concentration dependent manner. Wild type cells (*ade6-M210 leu1-32 ura4-D18*) were synchronised in G2 by lactose gradient centrifugation²⁹ and released into rich medium (3% glucose, 0.5% yeast extract, 100mg/L adenine) without (UT = untreated) or with 10µM of the indicated haloacetonitriles (HANs). All HANs were diluted from a 12mM stock solution in DMSO. **(a)** bromoacetonitrile (BAN), **(b)** chloroacetonitrile (CAN), **(c)** dichloroacetonitrile (DCAN), **(d)** dibromoacetonitrile (DBAN), **(e)** trichloroacetonitrile (TCAN), **(f)** DBAN at 10µM or 20µM, respectively. **(g)** DBAN affects cells in S phase which triggers a second cycle delay.

Figure 2. DBAN and TCAN delay G1-S transition

(a) Wild type cells without auxotrophic markers were synchronised in G1 by nitrogen starvation in minimal medium (3% glucose, 0.67% nitrogen base w/o amino acids and ammonium sulphate) at 30°C²⁹. Cells were washed and released at T=0h into pre-warmed minimal medium with ammonium sulphate. Samples were withdrawn at the indicated time points and the DNA content was measured by flow cytometry²⁹. The dotted lines indicate 1 copy of the chromosomes (1C, G1) and two copies (2C, G2), respectively. **(b)** Comparison of the DNA content at the start of the experiment (0h, green histogram) with the DNA content 4h after release (red histogram). Cells were released into medium with 10µM of the indicated haloacetonitriles or 15mM hydroxyurea (HU). **(c)** Comparison of the DNA content 8h post-release. The blue histogram is the DNA content of untreated cells (UT) and the red histogram is the DNA content of cells treated with the indicated chemicals. Nitrogen starvation arrests cells in G1 before start, whereas HU arrests cells in

early S phase.

Figure 3. DBAN kills cells mutated in DNA polymerase delta

(a) Model of the replication fork (adapted from ²²). **(b-e)** Serial dilutions of the indicated strains were applied to rich medium plates at 30°C. One plate was incubated at 37°C. Incubation time: 3 days. The final concentration of DBAN was 10µM, but 20µM for TCAN. The mutant alleles are: pol alpha (*swi7.H4*), Ctf4 (*mcl1-1*), pol delta (*cdc6.23*, *cdc27.P11*, *cdc1.p13*), pol epsilon (*cdc20.M10*), S phase cell cycle inhibitor Mik1 (*mik1::ura4+*), cell cycle inhibitor Wee1 (*wee1::ura4+*), $\Delta cdm1$ (non-essential pol delta subunit, *cdm1::ura4+*), MCM2 (*cdc19.P1*), MCM4 (*cdc21-M68*), MCM5 (*nda4-108*), DDK/Cdc7 (*hsk1-1312*), Rad4 (TopBP1) (*rad4.116*), MAP kinase Sty1 (*sty1::ura4+*). Final concentration of BAN, CAN and DCAN is 10µM.

Figure 4. DBAN advances DNA replication in a pol delta mutant

(a) Wild type cells (*ade6-M210 leu1-32 ura4-D18*) were grown in rich medium at 30°C and synchronised in early S phase for 3.5h in 15mM hydroxyurea (HU) ²⁹. HU was washed out and cells were released into pre-warmed rich medium. The DNA content was measured at the indicated times. The dotted lines indicate 1 copy of the chromosomes (1C, G1) and two copies (2C, G2), respectively. The DNA content of nitrogen starved cells (no N) was measured in a parallel experiment to have an internal standard. **(b-d)**. The indicated mutant strains were HU-synchronised and released into rich medium with or without 10µM DBAN. The green histogram is the DNA content of untreated cells, the red histogram is the DNA content in the presence of DBAN.

Figure 5. DBAN suppresses Chk1 phosphorylation

(a-b) *cds1-His₆HA₂* and *chk1-HA₃* cells were grown in rich medium at 30°C and treated for 4h with 10µM DBAN, 12µM camptothecin (CPT), 12mM hydroxyurea (HU) or the combination as indicated. Total protein extracts were loaded on a 6% phostag gel. H2AX phosphorylation at S129 was detected after electrophoresis on a 20% acrylamide (37.5:1 acrylamide:bisacrylamide) gel, whereas the Chk1 shift was detected after electrophoresis on a 10% (100:1 acrylamide:bisacrylamide) gel. The arrows indicate the smaller Cds1 band, Chk1-S345 phosphorylation and the hyper-phosphorylation of Chk1. **(c)** Model of Chk1 activation by Rad3 at broken replication forks. CPT immobilises Topoisomerase 1 and the Rad9-Rad1-Hus1 ring aids Chk1 phosphorylation. Rad9 is also phosphorylated by Rad3⁴⁰. **(d)** Drop test of the indicated strains. Chk1-D155E-HA3 is a kinase-dead mutant. DBAN: 10µM; CPT: 12µM. **(e-f)** *chk1-HA₃* cells were HU synchronised (3.5h, 15mM HU, rich medium) and released into medium without (UT) or with CPT (12µM), CPT (12µM) + DBAN (10µM) or CPT (12µM) + TCAN (10µM). Total protein extracts were separated on a 8% (Mrc1) and 10% (Chk1) acrylamide gel. P = Phospho-Chk1-S345 shift band). **(g)** *rad9-HA₃* cells were HU-synchronised and released into rich medium without (UT) or with CPT (12µM), DBAN (10µM) or CPT (12µM) + DBAN (10µM). P = Phospho-Rad9 shift band.

Figure 6. Model

(a) DBAN blocks G1-S transition. **(b)** DBAN prevents Chk1 phosphorylation by Rad3 at a broken fork. The details of the model are discussed in the main text.

Supplementary Figure 1.

(a-b) Wild type cells (*ade6-M210 leu1-32 ura4-D18*) were synchronised by lactose

gradient centrifugation in G2 and released into rich medium without (UT) or with 10µM DBAN (DB). (a) septated G1/S cells, (b) mitotic cells. (c) Checkpoint defective *rad3::ade6+ tel1::leu2+* cells. (d) Wild type cells were treated with 10µM of the indicated haloacetonitriles for 3h at 30°C. Phosphorylated H2AX-S129 was detected using a phosphospecific antibody. Cdc2 = loading control. (e) Concentration dependency of the decline in H2AX phosphorylation. (f) The indicated strains were G2-synchronised and exposed to 20µM DBAN. (g) *nda3.KM311* mutant cells were synchronised ³² at 20°C for 8h and released into rich medium at 30°C. The DNA content of the arrested cells (red) and of cells 70 min post-release (green) is shown. The arrow indicates G2 cells. (h) *chk1-HA₃* cells were treated with 0.05% MMS (methyl-methanesulfonate) or 12µM CPT with or without 10µM DBAN for 3h at 30°C. (i) phos-tag analysis of the Rad9 protein samples shown in figure 5g.

Supplementary Figure 2.

Wild type cells (*ade6-M210 leu1–32 ura4-D18*) were synchronised in early S for 3.5h with 15mM HU at 30°C and released into pre-warmed rich medium without a drug (a), with or without 10µM DBAN (b), with or without 10µM TCAN (c). The DNA content of the untreated cells (green) and of cells in the presence of the HAN (red) is shown. The dotted line indicates cells with a 2C (G2) DNA content.

Acknowledgements

We are grateful to George Meyrick for matched funding in support of the KESS (Knowledge Economy Skills Scholarships) Master project (F005714).

474 **Author Contributions**

475 TC wrote the manuscript, designed the study, performed most experiments and analysed
476 the data. JD performed some experiments. NF, CD and CF are co-applicants with TC on
477 the KESS grant and initiated the project. All authors reviewed the manuscript.

478

479 **References**

1. Jia, A., Wu, C. & Duan, Y. Precursors and factors affecting formation of haloacetonitriles and chloropicrin during chlor(am)ination of nitrogenous organic compounds in drinking water. *J. Hazard. Mater.* **308**, 411–418 (2016).
2. Bond, T., Templeton, M. R., Mokhtar Kamal, N. H., Graham, N. & Kanda, R. Nitrogenous disinfection byproducts in English drinking water supply systems: Occurrence, bromine substitution and correlation analysis. *Water Res.* **85**, 85–94 (2015).
3. Morris, R. D., Audet, A. M., Angelillo, I. F., Chalmers, T. C. & Mosteller, F. Chlorination, chlorination by-products, and cancer: a meta-analysis. *Am. J. Public Health* **82**, 955–963 (1992).
4. McGeehin, M. A., Reif, J. S., Becher, J. C. & Mangione, E. J. Case-control study of bladder cancer and water disinfection methods in Colorado. *Am. J. Epidemiol.* **138**, 492–501 (1993).
5. Cantor, K. P. *et al.* Drinking water source and chlorination byproducts in Iowa. III. Risk of brain cancer. *Am. J. Epidemiol.* **150**, 552–560 (1999).
6. Bull, R. J. *et al.* Evaluation of mutagenic and carcinogenic properties of brominated and chlorinated acetonitriles: by-products of chlorination. *Fundam. Appl. Toxicol. Off. J. Soc. Toxicol.* **5**, 1065–1074 (1985).
7. National Toxicology Program. Toxicology and carcinogenesis studies of dibromoacetonitrile (CAS No. 3252-43-5) in F344/N rats and B6C3F1 mice (drinking water studies). *Natl. Toxicol. Program Tech. Rep. Ser.* 1–193 (2010).
8. Hu, Y. *et al.* Detection of genotoxic effects of drinking water disinfection by-products using *Vicia faba* bioassay. *Environ. Sci. Pollut. Res. Int.* **24**, 1509–1517 (2017).
9. Muller-Pillet, V., Joyeux, M., Ambroise, D. & Hartemann, P. Genotoxic activity of five haloacetonitriles: comparative investigations in the single cell gel electrophoresis (comet) assay and the ames-fluctuation test. *Environ. Mol. Mutagen.* **36**, 52–58 (2000).
10. Lin, E. L., Daniel, F. B., Herren-Freund, S. L. & Pereira, M. A. Haloacetonitriles: metabolism, genotoxicity, and tumor-initiating activity. *Environ. Health Perspect.* **69**, 67–71 (1986).
11. Zhang, S.-H., Miao, D.-Y., Tan, L., Liu, A.-L. & Lu, W.-Q. Comparative cytotoxic and

- genotoxic potential of 13 drinking water disinfection by-products using a microplate-based cytotoxicity assay and a developed SOS/umu assay. *Mutagenesis* **31**, 35–41 (2016).
12. Jacob, S., Kaphalia, B. S., Jacob, N. & Ahmed, A. E. The water disinfectant byproduct dibromoacetonitrile induces apoptosis in rat intestinal epithelial cells: possible role of redox imbalance. *Toxicol. Mech. Methods* **16**, 227–234 (2006).
 13. Ahmed, A. E., Jacob, S., Nagy, A. A. & Abdel-Naim, A. B. Dibromoacetonitrile-induced protein oxidation and inhibition of proteasomal activity in rat glioma cells. *Toxicol. Lett.* **179**, 29–33 (2008).
 14. Poon, R., Chu, I., LeBel, G., Yagminas, A. & Valli, V. E. Effects of dibromoacetonitrile on rats following 13-week drinking water exposure. *Food Chem. Toxicol. Int. J. Publ. Br. Ind. Biol. Res. Assoc.* **41**, 1051–1061 (2003).
 15. Pereira, M. A., Lin, L. H. & Mattox, J. K. Haloacetonitrile excretion as thiocyanate and inhibition of dimethylnitrosamine demethylase: a proposed metabolic scheme. *J. Toxicol. Environ. Health* **13**, 633–641 (1984).
 16. Ahmed, A. E., Soliman, S. A., Loh, J. P. & Hussein, G. I. Studies on the mechanism of haloacetonitriles toxicity: inhibition of rat hepatic glutathione S-transferases in vitro. *Toxicol. Appl. Pharmacol.* **100**, 271–279 (1989).
 17. Abdel-Wahab, M. H., Arafa, H. M. M., El-Mahdy, M. A. & Abdel-Naim, A. B. Potential protective effect of melatonin against dibromoacetonitrile-induced oxidative stress in mouse stomach. *Pharmacol. Res.* **46**, 287–293 (2002).
 18. Komaki, Y., Mariñas, B. J. & Plewa, M. J. Toxicity of drinking water disinfection byproducts: cell cycle alterations induced by the monohaloacetonitriles. *Environ. Sci. Technol.* **48**, 11662–11669 (2014).
 19. Tognetti, S., Riera, A. & Speck, C. Switch on the engine: how the eukaryotic replicative helicase MCM2-7 becomes activated. *Chromosoma* **124**, 13–26 (2015).
 20. Yabuuchi, H. *et al.* Ordered assembly of Sld3, GINS and Cdc45 is distinctly regulated by DDK and CDK for activation of replication origins. *EMBO J.* **25**, 4663–4674 (2006).
 21. Masai, H. *et al.* Phosphorylation of MCM4 by Cdc7 kinase facilitates its interaction with Cdc45

- on the chromatin. *J. Biol. Chem.* **281**, 39249–39261 (2006).
22. Georgescu, R. *et al.* Structure of eukaryotic CMG helicase at a replication fork and implications to replisome architecture and origin initiation. *Proc. Natl. Acad. Sci. U. S. A.* **114**, E697–E706 (2017).
 23. Xu, Y., Davenport, M. & Kelly, T. J. Two-stage mechanism for activation of the DNA replication checkpoint kinase Cds1 in fission yeast. *Genes Dev.* **20**, 990–1003 (2006).
 24. Tanaka, K. & Russell, P. Mrc1 channels the DNA replication arrest signal to checkpoint kinase Cds1. *Nat. Cell Biol.* **3**, 966–972 (2001).
 25. Matsumoto, S. *et al.* Checkpoint-Independent Regulation of Origin Firing by Mrc1 through Interaction with Hsk1 Kinase. *Mol. Cell. Biol.* **37**, (2017).
 26. Wan, S., Capasso, H. & Walworth, N. C. The topoisomerase I poison camptothecin generates a Chk1-dependent DNA damage checkpoint signal in fission yeast. *Yeast Chichester Engl.* **15**, 821–828 (1999).
 27. Lindsay, H. D. *et al.* S-phase-specific activation of Cds1 kinase defines a subpathway of the checkpoint response in *Schizosaccharomyces pombe*. *Genes Dev.* **12**, 382–395 (1998).
 28. Gaillard, H., García-Muse, T. & Aguilera, A. Replication stress and cancer. *Nat. Rev. Cancer* **15**, 276–289 (2015).
 29. Luche, D. D. & Forsburg, S. L. Cell-cycle synchrony for analysis of *S. pombe* DNA replication. *Methods Mol. Biol. Clifton NJ* **521**, 437–448 (2009).
 30. al-Khodairy, F. *et al.* Identification and characterization of new elements involved in checkpoint and feedback controls in fission yeast. *Mol. Biol. Cell* **5**, 147–160 (1994).
 31. Rozenzhak, S. *et al.* Rad3 decorates critical chromosomal domains with gammaH2A to protect genome integrity during S-Phase in fission yeast. *PLoS Genet.* **6**, e1001032 (2010).
 32. Hiraoka, Y., Toda, T. & Yanagida, M. The NDA3 gene of fission yeast encodes beta-tubulin: a cold-sensitive *nda3* mutation reversibly blocks spindle formation and chromosome movement in mitosis. *Cell* **39**, 349–358 (1984).
 33. Francesconi, S., Grenon, M., Bouvier, D. & Baldacci, G. p56(chk1) protein kinase is required for the DNA replication checkpoint at 37 degrees C in fission yeast. *EMBO J.* **16**, 1332–1341

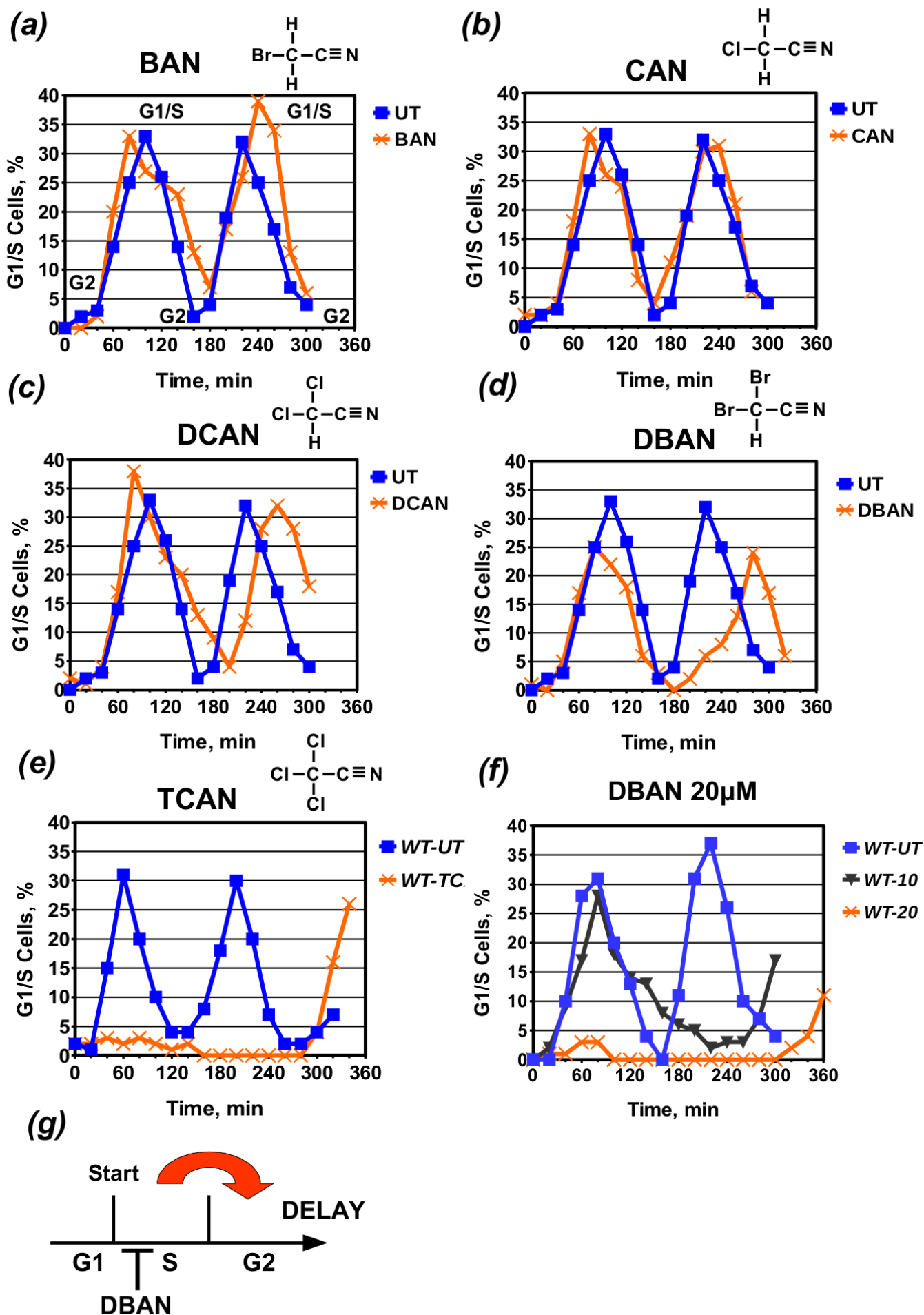
(1997).

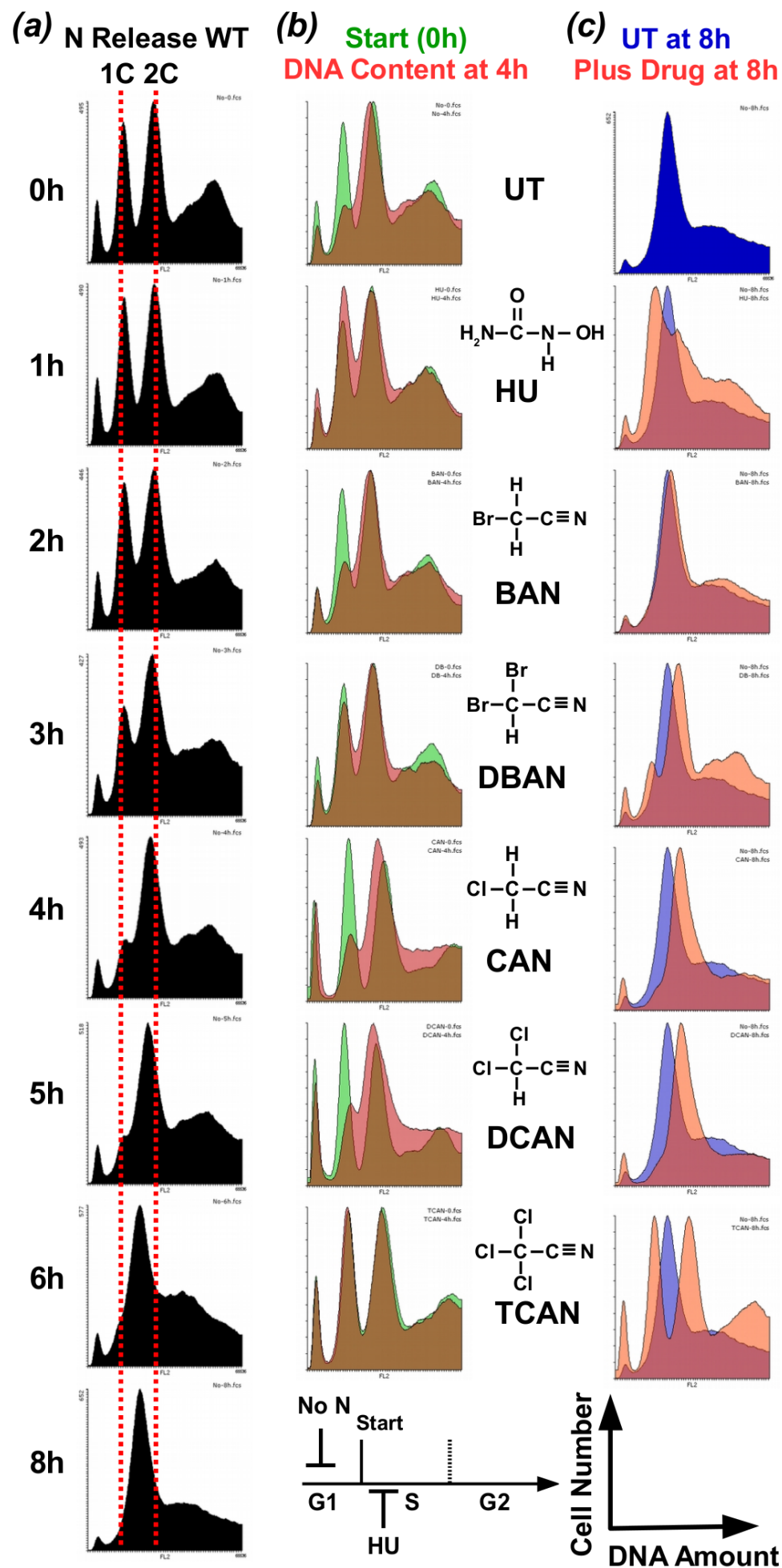
34. Bermudez, V. P., MacNeill, S. A., Tappin, I. & Hurwitz, J. The influence of the Cdc27 subunit on the properties of the *Schizosaccharomyces pombe* DNA polymerase delta. *J. Biol. Chem.* **277**, 36853–36862 (2002).
35. Aono, N., Sutani, T., Tomonaga, T., Mochida, S. & Yanagida, M. Cnd2 has dual roles in mitotic condensation and interphase. *Nature* **417**, 197–202 (2002).
36. Kinoshita, E., Kinoshita-Kikuta, E., Takiyama, K. & Koike, T. Phosphate-binding tag, a new tool to visualize phosphorylated proteins. *Mol. Cell. Proteomics MCP* **5**, 749–757 (2006).
37. Walworth, N. C. & Bernards, R. rad-dependent response of the chk1-encoded protein kinase at the DNA damage checkpoint. *Science* **271**, 353–356 (1996).
38. Kosoy, A. & O’Connell, M. J. Regulation of Chk1 by its C-terminal domain. *Mol. Biol. Cell* **19**, 4546–4553 (2008).
39. Redon, C. *et al.* Yeast histone 2A serine 129 is essential for the efficient repair of checkpoint-blind DNA damage. *EMBO Rep.* **4**, 678–684 (2003).
40. Furuya, K., Poitelea, M., Guo, L., Caspari, T. & Carr, A. M. Chk1 activation requires Rad9 S/TQ-site phosphorylation to promote association with C-terminal BRCT domains of Rad4TOPBP1. *Genes Dev.* **18**, 1154–1164 (2004).
41. Caspari, T. *et al.* Characterization of *Schizosaccharomyces pombe* Hus1: a PCNA-related protein that associates with Rad1 and Rad9. *Mol. Cell. Biol.* **20**, 1254–1262 (2000).
42. Kurose, A. *et al.* Effects of hydroxyurea and aphidicolin on phosphorylation of ataxia telangiectasia mutated on Ser 1981 and histone H2AX on Ser 139 in relation to cell cycle phase and induction of apoptosis. *Cytom. Part J. Int. Soc. Anal. Cytol.* **69**, 212–221 (2006).
43. Nakamura, T. M., Du, L.-L., Redon, C. & Russell, P. Histone H2A phosphorylation controls Crb2 recruitment at DNA breaks, maintains checkpoint arrest, and influences DNA repair in fission yeast. *Mol. Cell. Biol.* **24**, 6215–6230 (2004).
44. Saka, Y., Esashi, F., Matsusaka, T., Mochida, S. & Yanagida, M. Damage and replication checkpoint control in fission yeast is ensured by interactions of Crb2, a protein with BRCT motif, with Cut5 and Chk1. *Genes Dev.* **11**, 3387–3400 (1997).

45. Li, X., Nan, A., Xiao, Y., Chen, Y. & Lai, Y. PP2A-B56 ϵ complex is involved in dephosphorylation of γ -H2AX in the repair process of CPT-induced DNA double-strand breaks. *Toxicology* **331**, 57–65 (2015).
46. Fukuura, M. *et al.* CDK promotes interactions of Sld3 and Drc1 with Cut5 for initiation of DNA replication in fission yeast. *Mol. Biol. Cell* **22**, 2620–2633 (2011).
47. Harris, S. *et al.* Delineating the position of rad4⁺/cut5⁺ within the DNA-structure checkpoint pathways in *Schizosaccharomyces pombe*. *J. Cell Sci.* **116**, 3519–3529 (2003).
48. Furuya, K. *et al.* DDK phosphorylates checkpoint clamp component Rad9 and promotes its release from damaged chromatin. *Mol. Cell* **40**, 606–618 (2010).
49. Chini, C. C. S. & Chen, J. Human claspin is required for replication checkpoint control. *J. Biol. Chem.* **278**, 30057–30062 (2003).
50. Carr, A. M., Moudjou, M., Bentley, N. J. & Hagan, I. M. The chk1 pathway is required to prevent mitosis following cell-cycle arrest at ‘start’. *Curr. Biol. CB* **5**, 1179–1190 (1995).
51. Ge, X. Q. & Blow, J. J. Chk1 inhibits replication factory activation but allows dormant origin firing in existing factories. *J. Cell Biol.* **191**, 1285–1297 (2010).
52. Sirimulla, S., Bailey, J. B., Vegesna, R. & Narayan, M. Halogen Interactions in Protein–Ligand Complexes: Implications of Halogen Bonding for Rational Drug Design. *J. Chem. Inf. Model.* **53**, 2781–2791 (2013).
53. Kortagere, S., Ekins, S. & Welsh, W. J. Halogenated ligands and their interactions with amino acids: implications for structure-activity and structure-toxicity relationships. *J. Mol. Graph. Model.* **27**, 170–177 (2008).
54. Elder, R. T. *et al.* HIV-1 Vpr induces cell cycle G2 arrest in fission yeast (*Schizosaccharomyces pombe*) through a pathway involving regulatory and catalytic subunits of PP2A and acting on both Wee1 and Cdc25. *Virology* **287**, 359–370 (2001).
55. Liew, D., Linge, K. L. & Joll, C. A. Formation of nitrogenous disinfection by-products in 10 chlorinated and chloraminated drinking water supply systems. *Environ. Monit. Assess.* **188**, 518 (2016).
56. Nakazawa, N., Mehrotra, R., Ebe, M. & Yanagida, M. Condensin phosphorylated by the

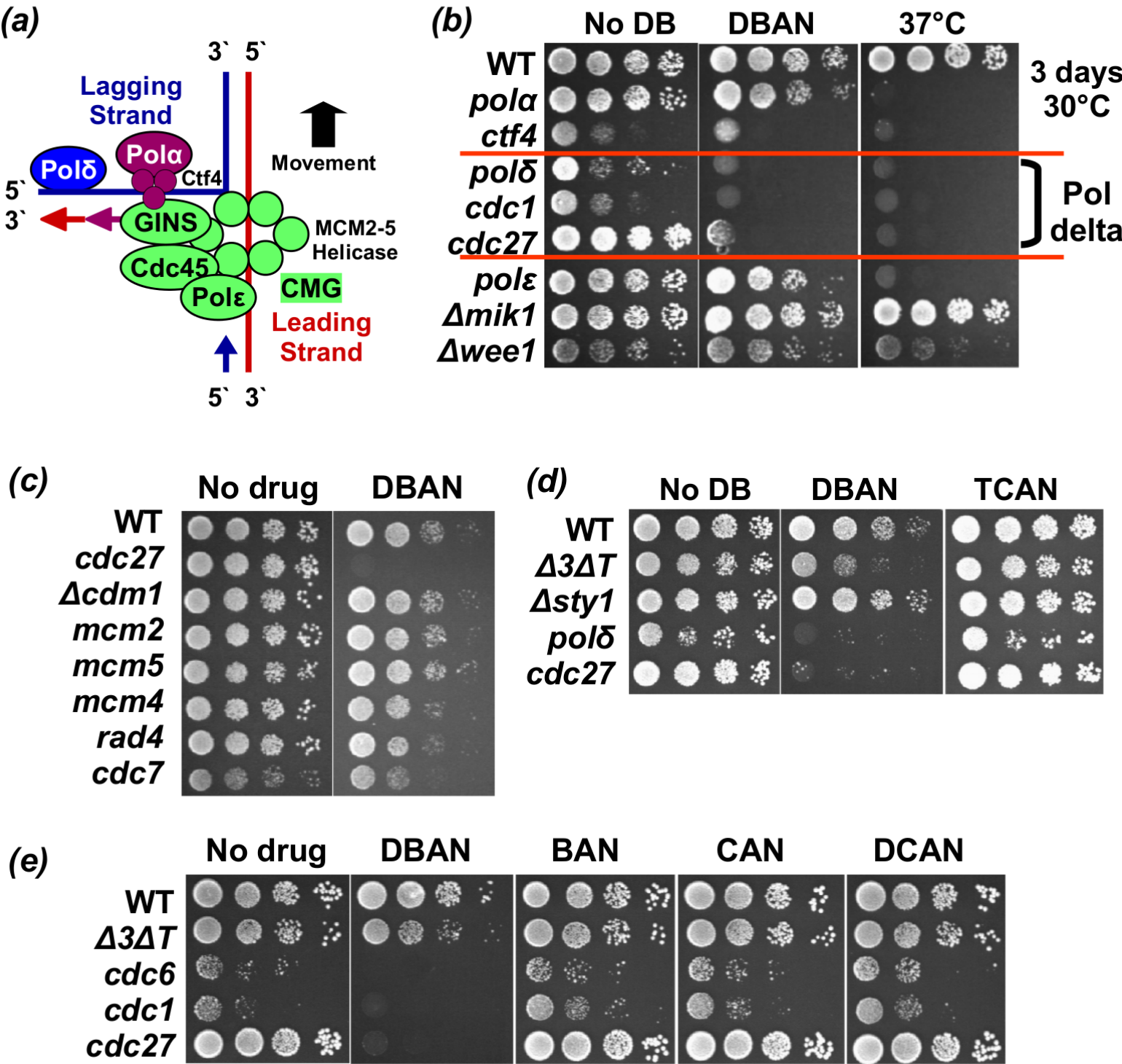
Aurora-B-like kinase Ark1 is continuously required until telophase in a mode distinct from Top2. *J. Cell Sci.* **124**, 1795–1807 (2011).

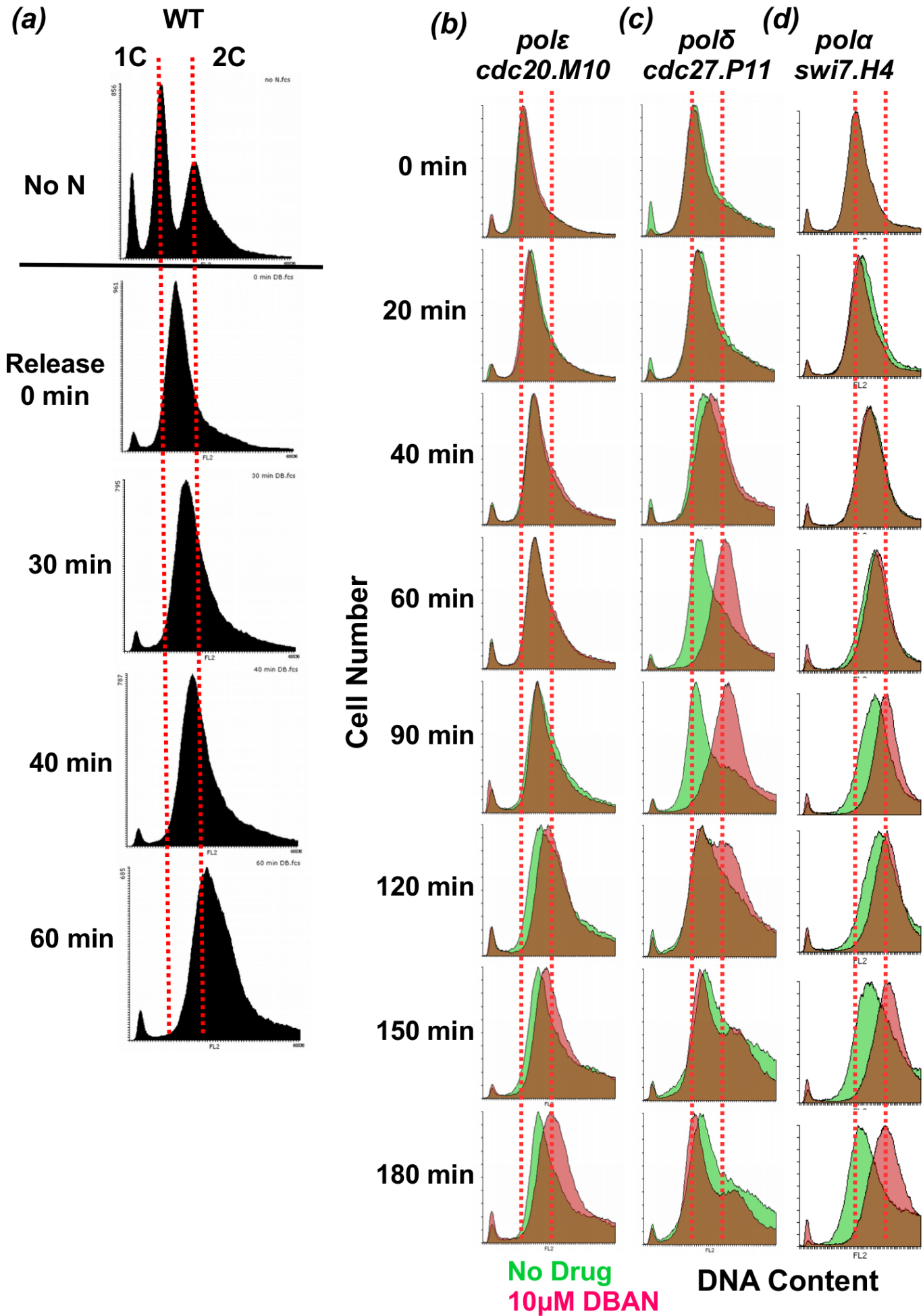
57. Caspari, T. & Hilditch, V. Two Distinct Cdc2 Pools Regulate Cell Cycle Progression and the DNA Damage Response in the Fission Yeast *S.pombe*. *PloS One* **10**, e0130748 (2015).



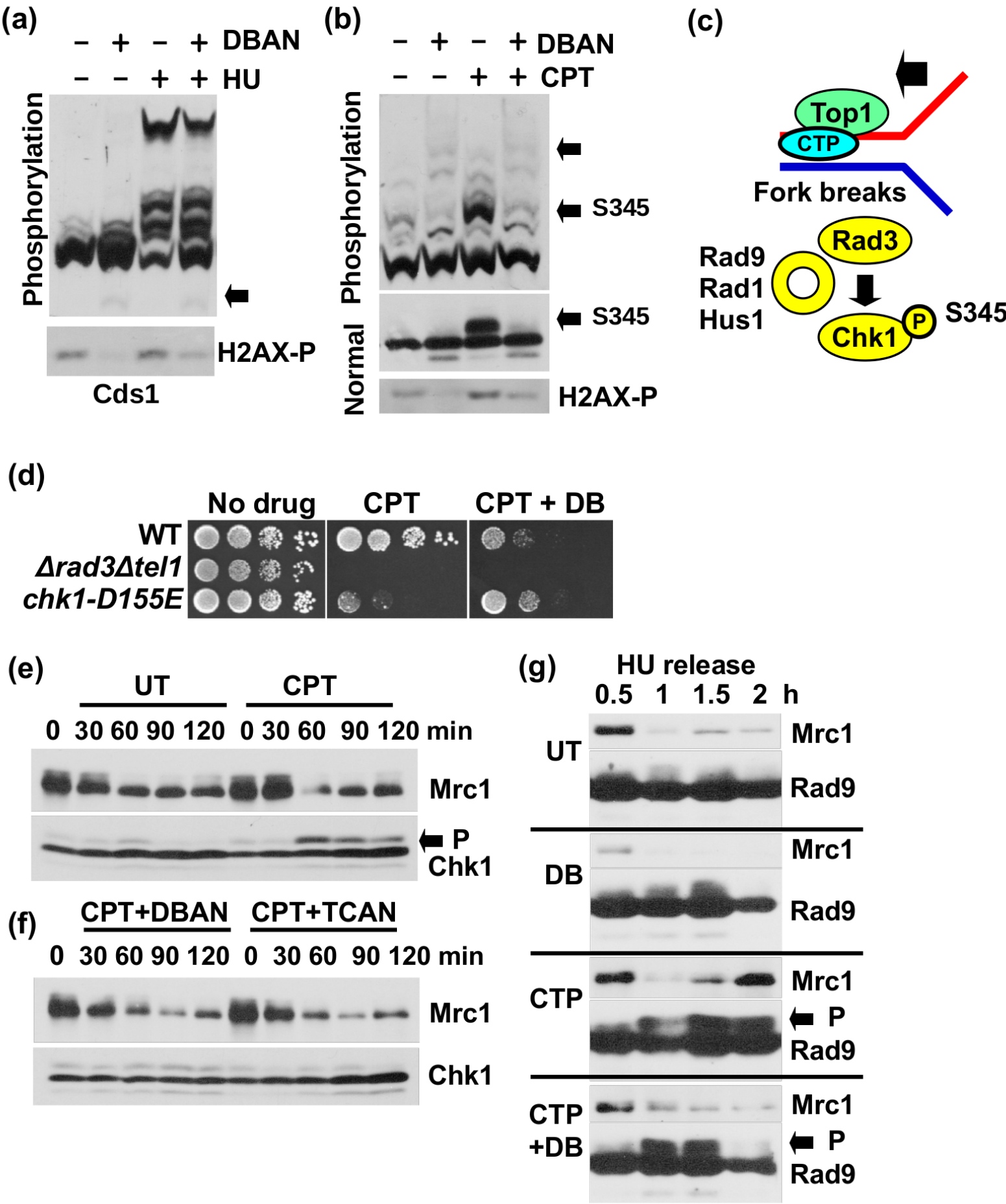


Caspari et al Fig 3 DNA polymerase delta mutants are DBAN sensitive





Caspari et al Fig 5 DBAN suppresses Chk1 activation



Caspari et al Figure 6

